The Canadian Journal of Statistics | La revue canadienne de statistique
Vol. 000, No. 00, 2025, e70038

Playing with fire? A mean-field game analysis of fire sales and systemic risk under regulatory capital constraints

Rüdiger FREY @, **Theresa TRAXLER**
Institute for Statistics and Mathematics, WU Vienna University of Economics and Business, Vienna, Austria

Abstract We analyze the effect of regulatory capital constraints on financial stability in a large homogeneous banking system using a mean-field game (MFG) model. Each bank holds cash and a tradable risky asset. Banks choose absolutely continuous trading rates in order to maximize expected terminal equity, with trades subject to transaction costs. Capital regulation requires equity to exceed a fixed multiple of the position in the tradable asset; breaches trigger forced liquidation. The asset drift depends on changes in average asset holdings across banks, so aggregate de-leveraging creates contagion effects, leading to an MFG. We discuss the coupled forward-backward partial differential equation (PDE) system characterizing equilibria of the MFG and solve the constrained MFG numerically. Experiments demonstrate that capital constraints accelerate de-leveraging and limit risk-bearing capacity. In some regimes, simultaneous breaches trigger liquidation cascades. Finally, we discuss several policy mechanisms for enhancing financial stability.

Résumé Nous analysons l'effet des contraintes de capital réglementaire sur la stabilité financière dans un grand système bancaire à l'aide d'une formulation en jeu à champ moyen (JCM). Chaque banque détient de la liquidité et un actif risqué négociable. Les banques choisissent des vitesses de négociation absolument continues afin de maximiser l'espérance de leur valeur terminale, sous des coûts de transaction. La régulation impose que les fonds propres dépassent un multiple fixé de l'actif négociable; toute violation entraîne une liquidation forcée. La dérive de l'actif dépend des positions moyenness, de sorte que le désendettement agrégé engendre des effets de contagion, menant à un JCM. Nous discutons le système d'EDP couplées caractérisant les équilibres du JCM, et nous résolvons le JCM contraint numériquement. Les expériences montrent que les contraintes accélèrent le désendettement et réduisent la capacité de portage du risque. Dans certains régimes, des violations simultanées déclenchent des cascades de liquidation. Enfin, nous étudions plusieurs mécanismes pour renforcer la stabilité financière.

Keywords Mean-field games; McKean–Vlasov equation; regulatory capital constraints; systemic risk.
MSC2020 Primary: 91G45; Secondary: 91A16.
@ Corresponding author ruediger.frey@wu.ac.at

1 Introduction

Contagious interactions between financial institutions play an important role in the amplification of economic shocks during a financial crisis. A prime example is the 2008–2009 global financial crisis, where comparatively small losses on the market for US subprime mortgages were magnified by the financial system and caused a major recession whose repercussions were felt across the world. This has led to a large body of literature on financial contagion and systemic risk. Most of this work focuses on *direct contagion* generated by contractual links between financial institutions such as interbank lending or over-the-counter (OTC) derivatives. Examples of this line of research include Eisenberg and Noe (2001), Elsinger et al. (2006), Rogers and Veraart (2013), Glasserman and Young (2016), and Frey and Hledik (2018). *Indirect* or *price-mediated contagion*, on the other

DOI: 10.1002/cjs.70038

hand, is caused by price effects due to forced de-leveraging, where a distressed financial institution is rapidly selling some of its risky assets in so-called fire sales in order to stay solvent or to comply with regulatory constraints. Typically, these fire sales exhaust demand for risky assets, which pushes asset prices downward and leads to losses at other financial institutions. The relevance of price-mediated contagion is stressed in many reports and policy papers on financial regulation. For instance, Daníelsson et al. (2001) discuss the endogeneity of financial risk and the role of liquidity with the Basel II regulation; contributions dealing with the 2008–2009 financial crisis include Hanson et al. (2011), Braouezec and Wagalath (2019), and several reports by the Basel committee. In particular, in Basel Committee on Banking Supervision (2014), the Basel committee acknowledges that

> at the height of the crisis financial markets forced the banking sector to reduce its leverage in a manner that amplified downward pressures on asset prices. This de-leveraging process exacerbated the feedback loop between losses, falling bank capital and shrinking credit availability.

Regulatory capital constraints can significantly amplify price-mediated contagion. In fact, under the Basel capital adequacy framework, a bank's risk capital (comprising equity and certain long-term debt instruments) must exceed a fixed multiple of its *risk-weighted assets*—a measure of asset size adjusted for risk. Substantial losses can reduce a bank's capital below the regulatory threshold. Because issuing new equity is typically costly, banks may resort to fire sales to restore compliance and avoid penalties or liquidation. In a downturn where many banks face losses simultaneously, these fire sales can propagate distress through price-mediated contagion, threatening financial stability. This mechanism is widely discussed in the macroprudential regulation literature; see, for example, Hanson et al. (2011). However, only a limited number of mathematical models explicitly examine the impact of regulatory capital constraints on systemic risk. These contributions are reviewed in Section 1.1.

In this article, we analyze price-mediated contagion within a model for a large, homogeneous banking system. In our setup, a bank may invest in two bank-specific risky assets, a non-tradable asset (e.g., retail loans) and a tradable asset (e.g., traded credit positions), and cash. The bank aims to maximize the expected value of its equity at a fixed terminal date. Trading in the tradable risky asset is subject to liquidity constraints, allowing only absolutely continuous strategies with finite trading rates. Transaction costs increase quadratically with the trading rate, making rapid portfolio adjustments prohibitively expensive. To capture regulatory capital constraints, we assume that a bank's equity must always exceed a fixed proportion of its asset holdings. Violation of this constraint triggers regulatory intervention and forced liquidation of the bank's assets.

Crucially, the expected return (drift) of each bank's tradable risky asset depends on the rate of change in the average holdings of the tradable risky assets across the banking system. When banks collectively reduce their positions—either voluntarily or through liquidation—expected returns decline, leading to price-mediated contagion. This feedback might arise from supply effects (outside investors must absorb greater supply) or informational effects (investors infer deteriorating fundamentals). Strategic interaction arises in this context because each bank's optimal trading rate depends on the drift of its tradable asset, which is itself influenced by the aggregate behaviour of all banks. While each bank is individually small and treats the asset drift as exogenous, in an equilibrium of the model the perceived drift used in computing the optimal trading strategy must coincide with the drift induced by the collective trading strategies, which adds a consistency condition. In economic terms, this corresponds to the notion of a *Nash equilibrium*, where each bank's strategy is optimal given the behaviour of all other banks in the system. Mathematically, the framework of this article corresponds to a *mean-field game* (MFG) formulation, where each agent is infinitesimally small and where agents interact through the distribution of their states (here the equity values and the and asset positions), analogously to mean-field interaction in statistical physics.

In the absence of capital constraints, the mathematical structure of our model aligns with the MFG framework of Cardaliaguet and LeHalle (2018), who analyze strategic interactions in optimal portfolio execution. As in their work, the coupled partial differential equation (PDE) system—comprising the dynamic programming equation for individual banks and the forward equation for the distribution of bank characteristics—can be reduced to a system of ordinary differential equations (ODEs) with an explicit solution. When capital constraints are introduced, however, the analysis is substantially more complex. The PDE system becomes a boundary value problem for which no explicit solution exists, necessitating numerical methods. Solving the PDE system associated with an MFG is particularly challenging, as it involves both forward and backward

components and thus requires solving a fixed-point problem. For our MFG model, we employ Picard iterations combined with a specialized discretization scheme inspired by Achdou and Laurière (2020).

Using this scheme, we study numerically the impact of capital constraints on the stability of the banking system. We find that banks liquidate their position faster than in the unregulated case, in particular when they are close to the liquidation boundary. Moreover, they hold, on average, a lower amount of the risky asset, so that the risk-bearing capacity of the banking system is reduced by the capital constraints. For certain parameter values, we observe a *liquidation cascade*, where many banks are violating the risk capital constraints more or less simultaneously and where the ensuing fire sales have a substantial impact on the drift of the risky assets. These results strengthen the regulatory literature's claim that capital constraints can trigger price-mediated contagion. Finally, we assess several macroprudential risk management policies—regulatory tools designed with the intention to limit the systemic effects of rapid, multi-institution de-leveraging—proposed in the literature (see Hanson et al. (2011)). Within our framework, the adverse effects of capital constraints vanish when the banking sector is adequately capitalized. Moreover, financial stability improves if banks breaching capital requirements are resolved in ways that curb price-mediated contagion, such as transferring assets to a special-purpose vehicle that is unwound gradually over time.

The remainder of the article is organized as follows. In Section 2, we introduce our setup and the optimization problem of an individual bank. The case without capital constraints, where the MFG has an explicit solution, is studied in Section 3. In Section 4, we discuss the PDE system for the MFG model with capital constraints. Numerical experiments studying the implications of capital constraints for financial stability are discussed in Section 5.

1.1 Literature review

We now review some of the related literature. In the absence of capital constraints, the mathematical structure of our model aligns with those employed in the analysis of optimal portfolio execution; see, for example, Cardaliaguet and LeHalle (2018), Casgrain and Jaimungal (2020), or the book Cartea et al. (2015).

Next, we turn to the literature on regulatory capital constraints in formal economic models. Braouezec and Wagalath (2018) develop a deterministic model of a single bank subject to risk-based capital requirements and examine its optimal liquidation strategy following an adverse shock to asset values. They show that, when price impact is present, capital constraints may trigger asset sales that drive an otherwise solvent bank into default. Crucially, the destabilizing mechanism operates through balance sheet dynamics rather than interbank contagion. Building on this line of research, Braouezec and Wagalath (2019) analyze a one-period model with finitely many banks holding a common risky asset. Following an exogenous shock at time $t = 1$, each bank liquidates the minimum quantity of assets required to satisfy Basel capital requirements. Market illiquidity renders these fire sales mutually reinforcing, giving rise to a strategic liquidation game. The authors prove the existence of equilibrium and, using simulations calibrated to the US banking system, demonstrate that price-mediated contagion can substantially amplify the initial shock. Feinstein (2020) extends this framework to continuous time with deterministic asset prices; see also Banerjee and Feinstein (2021). In these models, banks respond passively to capital requirements. By contrast, our approach integrates regulatory constraints and price-mediated contagion directly into banks' dynamic portfolio decisions, shaping behaviour even before liquidation becomes necessary. For further contributions on fire sales and price-mediated contagion, see Cont and Wagalath (2016), Cont and Schaanning (2019), and the references therein.

We conclude by reviewing mean-field models that address systemic risk. An early contribution in this direction is Carmona et al. (2015). Further studies closely related to our analysis include Nadtochiy and Shkolnikov (2019), Hambly et al. (2019), Hambly and Søjmark (2019), Ledger and Søjmark (2020), and Cuchiero et al. (2023). These works extend the neuron-firing model of Delarue et al. (2015) to a systemic risk setting, focusing on homogeneous banking networks in which each institution holds a fixed position in a risky asset and experiences losses whenever another institution's asset value crosses a default threshold. The asymptotic behaviour as the number of banks $m \to \infty$ is investigated, leading to a characterization in terms of the associated McKean–Vlasov dynamics, that is, the (stochastic) PDE governing the distribution of banks' states. The contagion mechanism underlying these mean-field models is conceptually aligned with the framework considered in this article, and we draw upon insights from Delarue et al. (2015) and Hambly et al. (2019) to interpret our numerical results on liquidation cascades.

While the aforementioned papers assume fixed bank positions, recent research investigates the optimal control of such systems from the perspective of a central planner (e.g., a regulator) who may inject capital into selected banks or influence the drift of their asset values. For example, Cuchiero et al. (2024)

develop a mean-field model of systemic bank defaults in which a regulator controls the drift of banks' equity processes—formulated as a drift-controlled supercooled Stefan problem—to design optimal bailout strategies. Similarly, Hambly and Jettkant (2023) and Bayraktar et al. (2023) study McKean–Vlasov control problems in mean-field systemic risk models. From an economic perspective, these works adopt the viewpoint of a central planner who enforces coordination between banks, whereas the present article focuses on strategic interaction and Nash equilibria.

The general literature on MFGs is by now large and growing fast. Fundamental contributions include Lasry and Lions (2006a, 2006b) and Carmona and Delarue (2018). Lasry and Lions (2006a, 2006b) focus on the PDE approach, whereas Carmona and Delarue (2018) discuss the probabilistic approach based on forward-backward stochastic differential equations (SDEs). Campi and Fischer (2018) provide first theoretical results on MFGs with absorption, where the state process of players is stopped upon hitting the boundary of a given set of admissible states—as in the present article. A good general introduction to the PDE approach for MFGs is given in Cardaliaguet and Porretta (2019).

2 The model

2.1 The banking system

Fix some horizon date T and a probability space $(\Omega, \mathcal{F}, \Pr)$. We consider a stylized banking system with a continuum I of identical banks. This model can be interpreted as limit for $N \to \infty$ of a finite system with N homogeneous banks. Each bank $i \in I$ holds some non-tradable risky asset with value A^i, for instance, retail loans. Moreover, it invests into a tradable risky asset S^i, for instance, tradable credit positions, and in cash. Trading in S^i is subject to liquidity constraints, allowing only absolutely continuous strategies with finite *trading rate* $\boldsymbol{\nu} = (\nu_t)_{0\le t\le T}$. Let $Q^i = (Q^i_t)_{0\le t\le T}$ denote the inventory process of tradable risky assets held by bank i, and let $C^i = (C^i_t)_{0\le t\le T}$ denote its corresponding cash position. We allow for $C^i_t < 0$, representing a net borrowing position—typical for highly leveraged banks—and, for simplicity, assume a zero interest rate, $r = 0$. For a fixed trading strategy $\boldsymbol{\nu}$, the dynamics of the processes (A^i, Q^i, S^i) are given by

$$\begin{aligned} \mathrm{d}A^i_t &= \sigma_A \mathrm{d}W^{A,i}_t \\ \mathrm{d}Q^i_t &= \nu_t \mathrm{d}t + \sigma_Q \mathrm{d}W^{Q,i}_t \\ \mathrm{d}S^i_t &= (\mu_{\mathrm{ex}} + \alpha\bar{\mu}_t)\mathrm{d}t + \sigma_S \mathrm{d}W^{S,i}_t, \end{aligned} \tag{1}$$

where $\alpha, \sigma_A, \sigma_S, \sigma_Q > 0$, and where $\mathbf{W}^i = (W^{Q,i}, W^{A,i}, W^{S,i})$ is a three-dimensional standard Brownian motion. The Brownian motions $\mathbf{W}^i$, $i \in I$ are assumed to be independent. The drift of S^i consists of two components: a constant exogenous trend μ_{ex}, and an *interaction* or *contagion term* $\bar{\mu}_t$. We assume that $\bar{\mu}_t$ equals the rate of change in the average holdings of the tradable risky assets across the banking system so that the drift of S^i declines when banks collectively reduce their positions in the tradable assets. A mathematical definition of $\bar{\mu}_t$ is deferred to equation (10) (for the case without capital constraints) and to (15) (for the case with capital constraints) since this necessitates some further concepts.

A trading strategy $\boldsymbol{\nu}$ is admissible for bank i if it is adapted to the filtration generated by the Brownian motion $\mathbf{W}^i$ and if it satisfies the integrability condition $\int_0^T (\nu_s)^2 \mathrm{d}s < \infty$. In order to penalize rapid position changes, we introduce transaction costs and assume that in implementing the strategy $\boldsymbol{\nu}$ a bank incurs instantaneous costs of size $\kappa\nu_t^2$ for some $\kappa > 0$. The cash account finances trading activities including transaction costs and records proceeds from asset sales. Its dynamics for a given strategy $\boldsymbol{\nu}$ are equal to

$$\mathrm{d}C^i_t = -S^i_t \mathrm{d}Q^i_t - \kappa\nu_t^2 \mathrm{d}t,$$

where the first term represents the cost of purchasing assets (for $\mathrm{d}Q^i_t > 0$) or the revenue from sales (for $\mathrm{d}Q^i_t < 0$), and the second term accounts for transaction costs.

We now discuss the dynamics described in (1) in greater detail. The diffusion term in the dynamics of Q^i reflects the inherent challenges large banks face in precisely managing their holdings of risky assets, because of factors such as execution delays. Both A^i and S^i follow arithmetic Brownian motions and may therefore take negative values. Although this is a simplification and not fully realistic, it significantly facilitates the analysis. To further streamline the exposition, the drift of the non-tradable asset A^i is assumed to be zero; this assumption can be relaxed without difficulty.

In our framework, contagion arises through more indirect channels than in standard fire sale models, where banks typically hold a common asset. Within the context of (1), contagion is primarily driven by supply-side effects or informational channels. For example, if the banking sector collectively reduces its asset holdings—either voluntarily or through forced liquidation—external investors must absorb the resulting excess supply. Additionally, if investors believe that banks possess superior information, collective asset sales by the banking sector may signal deteriorating fundamentals. Both mechanisms tend to exert downward pressure on the prices of all tradable assets.

Note, finally, that the Brownian motions $\mathbf{W}^i$, $i \in I$, are independent. Thus, banks interact only through the effect of their trading on the drift term $\bar{\mu}$. Introducing a common noise component into the dynamics of tradable asset prices—representing global economic shocks—would substantially complicate the model. In such a case, the distribution of bank characteristics becomes random and is governed by a stochastic partial differential equation (SPDE). We therefore leave this extension for future work. Systemic risk models of a mean-field type incorporating common noise include those of Hambly and Søjmark (2019), Ledger and Søjmark (2020), and Burzoni and Campi (2023).

2.2 The Hamilton–Jacobi–Bellman (HJB) equation

From now on, we omit the superscript i since the banks in our system are all identical. The *equity value* of a generic bank under the trading strategy $\boldsymbol{\nu}$, defined as the difference between assets and liabilities, is given by

$$X_t^{\boldsymbol{\nu}} = A_t + S_t Q_t^{\boldsymbol{\nu}} + C_t^{\boldsymbol{\nu}}.$$

We assume that each bank selects its trading rate $\boldsymbol{\nu}$ to maximize the expected terminal equity value $\mathrm{E}\big(X_T^{\boldsymbol{\nu}}\big)$ over all admissible strategies $\boldsymbol{\nu}$.

Next, we derive the dynamic programming or HJB equation for this optimization problem. Using Itô's product formula and the assumption that the Brownian motions are independent, we get the following dynamics for the process $\mathbf{X} = (Q, X)$:

$$\begin{aligned}
\mathrm{d}Q_t &= \nu_t \mathrm{d}t + \sigma_Q \mathrm{d}W_t^Q, \\
\mathrm{d}X_t &= \mathrm{d}A_t + \mathrm{d}(S_t Q_t) + \mathrm{d}C_t = \mathrm{d}A_t + Q_t \mathrm{d}S_t + S_t \mathrm{d}Q_t - S_t \mathrm{d}Q_t - \kappa \nu_t^2 \mathrm{d}t \\
&= \big(Q_t(\mu_{\mathrm{ex}} + \alpha \bar{\mu}_t) - \kappa \nu_t^2\big)\mathrm{d}t + \sigma_A \mathrm{d}W_t^A + Q_t \sigma_S \mathrm{d}W_t^S.
\end{aligned}$$

Consider a generic bank and assume that the bank takes a deterministic evolution $t \mapsto \mu(t)$ of the contagion term as given. Then, under a constant strategy $\nu_t \equiv \nu$, the process $\mathbf{X}$ is Markovian with generator

$$\mathcal{L}_{\mathbf{X}}^{\nu} f = \nu \partial_q f + \big(q(\mu_{\mathrm{ex}} + \alpha \mu(t)) - \kappa \nu^2\big)\partial_x f + \frac{1}{2}\sigma_Q^2 \partial_q^2 f + \frac{1}{2}\big(\sigma_A^2 + \sigma_S^2 q^2\big)\partial_x^2 f,$$

for f, a twice-differential function on $\mathbb{R}^2$. Standard arguments of stochastic control, see for instance Pham (2009, Chapter 3), give the following HJB equation for the value function u of the bank's optimization problem:

$$0 = \partial_t u + \sup_{\nu \in \mathbb{R}} \Big\{ \nu \partial_q u + \big(q(\mu_{\mathrm{ex}} + \alpha \mu) - \kappa \nu^2\big)\partial_x u + \frac{1}{2}\sigma_Q^2 \partial_q^2 u + \frac{1}{2}\big(\sigma_A^2 + \sigma_S^2 q^2\big)\partial_x^2 u \Big\}; \tag{2}$$

the terminal condition is $u(T, q, x) = x$. Moving the non-ν-dependent terms out of the supremum in (2) gives the following equivalent form of the HJB equation:

$$0 = \partial_t u + q(\mu_{\mathrm{ex}} + \alpha \mu(t))\partial_x u + \frac{1}{2}\sigma_Q^2 \partial_q^2 u + \frac{1}{2}\big(\sigma_A^2 + \sigma_S^2 q^2\big)\partial_x^2 u + \sup_{\nu \in \mathbb{R}} \{\nu \partial_q u - \kappa \nu^2 \partial_x u\}. \tag{3}$$

Suppose that (3) has a classical solution. In that case, the optimal trading rate is found by maximizing the last term in (3) with respect to ν. This yields the feedback control strategy $\boldsymbol{\nu}_t^* = \nu^*(t, Q_t, S_t)$, where

$$\nu^*(t, q, x) = \frac{\partial_q u(t, x, q)}{2\kappa \partial_x u(t, x, q)}. \tag{4}$$

In an equilibrium, $\mu(t)$ should coincide with the contagion term $\bar{\mu}_t$ resulting from the aggregate trading behaviour of all banks in the system. This adds the consistency or *equilibrium* condition $\mu(t) = \bar{\mu}_t$ to the model. This condition will be discussed in Sections 3 and 4.

2.3 Risk capital constraints

Under the Basel capital adequacy framework, a bank's risk capital must exceed a multiple of its *risk-weighted assets* (RWAs). This quantity is essentially a weighted average of asset positions, with weights reflecting risk levels; see, for example, McNeil et al. (2015). In this article, we consider a simplified representation of this requirement. First, we model the bank's risk capital at time t as its equity value X_t, which leads to the constraint $X_t > \tilde{\beta} RWA_t$. Second, we assume that RWA_t consists of two components: a fixed capital charge RWA^{A} for the constant position in the non-traded asset A representing the banking book, and a position-dependent capital charge RWA_t^{S} for the traded asset S, so that

$$\mathrm{RWA}_t = \mathrm{RWA}^{\mathrm{A}} + \mathrm{RWA}_t^{\mathrm{S}}.$$

Following standard risk management practices, the trading book capital charge is computed as the value at risk VaR_α for a high confidence level α of the change in portfolio value over a fixed risk horizon Δt (e.g., $\Delta t = 10$ days), assuming that the position remains unchanged over $[t, t+\Delta t]$, see McNeil et al. (2015, Chapter 2). This yields

$$\mathrm{RWA}_t^{\mathrm{S}} = \mathrm{VaR}_\alpha(Q_t(S_{t+\Delta t} - S_t)),$$

where the position Q_t is known at time t. Under the dynamics of S from (1), given Q_t, the random variable $Q_t(S_{t+\Delta t} - S_t)$ is approximately normally distributed with variance $\Delta t Q_t^2 \sigma_S^2$ (the mean can be ignored if Δt is small). Hence

$$\mathrm{RWA}_t^{\mathrm{S}} \approx \widehat{\mathrm{RWA}}_t^{\mathrm{S}} = \sqrt{\Delta t}\sigma_S q_\alpha |Q_t|,$$

where q_α is the α quantile of the standard normal distribution.

In the following formula, we replace $\mathrm{RWA}_t^{\mathrm{S}}$ with $\widehat{\mathrm{RWA}}_t^{\mathrm{S}}$. This leads to the following form of the capital adequacy constraint:

$$X_t > \tilde{\beta}(\mathrm{RWA}^{\mathrm{A}} + \widehat{\mathrm{RWA}}_t^{\mathrm{S}}) = \tilde{\beta}\mathrm{RWA}^{\mathrm{A}} + \tilde{\beta}\sqrt{\Delta t}\sigma_S q_\alpha |Q_t| =: \beta|Q_t| + c \tag{5}$$

for suitable constants $c, \beta > 0$. We remark that in the derivation of the capital constraint (5) one might use the expected shortfall or any other positive homogeneous and translation-invariant risk measure instead of VaR_α.

We denote the set of *acceptable positions* by the open set $\mathcal{A}$ with

$$\mathcal{A} = \{\mathbf{x} = (q, x) \in \mathbb{R} \times \mathbb{R}^+ : x > \beta|q| + c\},$$

and we denote its boundary by $\partial\mathcal{A}$. We assume that a bank is liquidated by the regulator at the stopping time $\tau = \inf\{t \geq 0 : \mathbf{X}_t \notin \mathcal{A}\}$, that is, liquidation happens as soon as the bank's position reaches $\partial\mathcal{A}$. Moreover, the equity holders lose their claim to the bank's equity in that case. The objective of the bank needs to be modified accordingly: with capital constraints a bank aims to maximize

$$\mathrm{E}\big(X_T^{\boldsymbol{\nu}} 1_{\{\tau > T\}}\big)$$

over all admissible strategies $\boldsymbol{\nu}$. This leads to the additional boundary condition $u \equiv 0$ on $\partial\mathcal{A}$ in the HJB equation. We refer to τ as the *liquidation time* of a bank and to $\partial\mathcal{A}$ as the *liquidation boundary*. Note that for numerical reasons, in Section 4 we consider a slightly relaxed version of the boundary condition on u.

3 The case without capital constraints

In this section, we derive an explicit solution for the optimal trading strategy and the resulting equilibrium drift in the absence of capital constraints (the so-called unregulated case). This sets the stage for the subsequent analysis of the case with capital constraints. Our analysis follows Cardaliaguet and LeHalle (2018), who analyze a model with similar structure in the context of optimal portfolio execution. We proceed in three steps.

Step 1

In this step, we study the value function for a given drift function drift $\mu(t)$. Denote the value function for the unregulated case by u^{unreg}. We make the assumption $u^{\mathrm{unreg}}(t, q, x) = x + v(t, q)$. This implies that $\partial_x u^{\mathrm{unreg}} = 1$ and we get the following HJB equation for v:

$$0 = \partial_t v + q(\alpha\mu(t) + \mu_{\mathrm{ex}}) + \sup_{\nu \in \mathbb{R}}\{\nu\partial_q v - \kappa\nu^2\}; \tag{6}$$

the terminal condition $u^{\text{unreg}}(T,q,x) = x$ leads to the condition $v(T,q) = 0$ for the function v. It follows that the optimal strategy is given by the function

$$\nu^*(t,q) = \frac{\partial_q v(t,q)}{2\kappa}, \tag{7}$$

in particular, ν^* is independent of x. Hence without capital constraints, the MFG model can analyzed purely in terms of the distribution of the inventory level Q. To determine the solution v, we make the assumption

$$v(t,q) = h_0(t) + h_1(t)q. \tag{8}$$

Now $\sup_{\nu\in\mathbb{R}}\{\nu\partial_q v - \kappa\nu^2\} = (\partial_q v)^2/(4\kappa)$. Substituting the form of v in (8) into the HJB equation (6) gives

$$0 = h_0' + h_1' q + q(\alpha\mu(t) + \mu_{\text{ex}}) + \frac{h_1^2}{4\kappa}.$$

This yields the following ODE system for h_0 and h_1:

$$h_1' = -\alpha\mu(t) - \mu_{\text{ex}} \text{ and } h_0' = -\frac{h_1^2}{4\kappa}, \tag{9}$$

with terminal conditions $h_0(T) = h_1(T) = 0$. It follows from (7) that the optimal strategy is given by $\nu^*(t,q) = h_1(t)/(2\kappa)$. Note that this strategy is independent of q, which is due to the very simple form of the terminal condition for u^{unreg}.

Step 2

We next examine the temporal evolution of the inventory-level distribution under the assumption that every bank employs the optimal trading strategy $\nu^*(t,q)$ and we discuss the contagion term $\bar{\mu}_t$. Let $m_t(\mathrm{d}q)$ denote the inventory-level distribution at time t. For any test function $f : \mathbb{R} \to \mathbb{R}$, define

$$\langle m_t, f\rangle := \int_{\mathbb{R}} f(q)\, m_t(\mathrm{d}q).$$

Since the Brownian motions driving the inventory dynamics are independent across banks, the measure $m_t(\mathrm{d}q)$ evolves in a fully deterministic fashion. In particular, there is no randomness in the evolution of m_t despite each bank's underlying noise, because these stochastic fluctuations average out in an infinitely large system. In this context, the average inventory level across the banking system equals $\langle m_t, q\rangle$, where, with a slight abuse of notation, we use the symbol q to denote the identity map $q \mapsto q$. Recall that the contagion term $\bar{\mu}_t$ is given by the rate of change of the average inventory level. Using the given notation, we may now give a formal definition for the case without capital constraints. We put

$$\bar{\mu}_t := \partial_t\langle m_t, q\rangle = \partial_t \int_{\mathbb{R}} q\, m_t(\mathrm{d}q). \tag{10}$$

Denote by $\mathcal{L}_Q$ the generator of Q given that the bank uses the feedback strategy $\nu^*(t,Q_t)$, that is,

$$\mathcal{L}_Q f = \nu^*(t,q)\partial_q f + \frac{1}{2}\sigma_Q^2\partial_q^2 f.$$

For f in the domain of $\mathcal{L}_Q$, the weak form of the forward equation for the evolution of the flow of measures $m_t(\mathrm{d}q)$ is

$$\partial_t\langle m_t, f\rangle = \langle m_t, \mathcal{L}_Q f\rangle. \tag{11}$$

If $m_t(\mathrm{d}q)$ admits a density, that is, if $m_t(\mathrm{d}q) = m(t,q)\mathrm{d}q$ for all t, the classical forward equation for the density $m(t,q)$ can be derived from (11) via integration by parts. However, this equation is not required in the unregulated case.

Next, we give an alternative representation for $\bar{\mu}_t$. Using the weak form of the forward equation and the fact that $\mathcal{L}_Q q = \nu^*$, we get that

$$\bar{\mu}_t = \partial_t\langle m_t, q\rangle = \langle m_t, \mathcal{L}_Q q\rangle = \langle m_t, \nu^*(t,\cdot)\rangle. \tag{12}$$

That is, without capital constraints, the contagion term $\bar{\mu}_t$ is equal to the average trading rate of the banks.

This relation warrants a discussion. In their study of MFGs for trade crowding, Cardaliaguet and LeHalle (2018) adopt the definition $\bar{\mu}_t = \langle m_t, \nu^*(t,\cdot)\rangle$. This is consistent with the literature on optimal portfolio execution, where the dependence of asset prices on trading rates is known as *permanent price impact*. In this paper, we use the definition $\bar{\mu}_t = \partial_t\langle m_t, q\rangle$, as this definition extends to the case with capital constraints. This point is further discussed in Section 4.2.1. Relation (12) also helps us to position our framework within the broader literature on MFGs. The definition $\bar{\mu}_t = \langle m_t, \nu^*(t,\cdot)\rangle$ yields, in the unregulated case, a formulation as a mean-field game of controls (MFGC), where agents interact through the joint distribution of their states and controls; this is the viewpoint taken in Cardaliaguet and LeHalle (2018). In contrast, the definition $\bar{\mu}_t = \partial_t\langle m_t, q\rangle$ corresponds to an MFG in which agents interact through the distribution of their states only. However, the coupling is non-standard, since the interaction at time t depends on the measure flow m_s for s in a neighbourhood of t, thus creating the need to compute $\partial_t\langle m_t, q\rangle$.

Step 3

Finally, we close the system and identify the equilibrium drift. Using (12), we get that

$$\bar{\mu}_t = \langle m_t, \nu^*(t,\cdot)\rangle = \frac{1}{2\kappa} h_1. \tag{13}$$

Recall that in equilibrium, the drift $\mu(t)$ used in the computation of the optimal strategy should coincide with the actual drift resulting from banks' trading activities; that is, we have the condition $\mu(t) = \bar{\mu}_t$. Using (9) and the relation (13), we therefore obtain the following ODEs for h_0 and h_1:

$$h_1' = -\frac{\alpha}{2\kappa} h_1 - \mu_{\text{ex}} \text{ and } h_0'^* = -\frac{h_1^2}{4\kappa},$$

with terminal condition $h_0(T) = h_1(T) = 0$. This leads to the following explicit solution:

$$h_0(t) = \frac{\kappa\mu_{\text{ex}}^2}{\alpha^3}\left[\alpha(T-t) + \kappa\left(e^{\frac{\alpha}{\kappa}(T-t)} - 4e^{\frac{\alpha}{2\kappa}(T-t)} + 3\right)\right],$$

$$h_1(t) = \frac{2\kappa\mu_{\text{ex}}}{\alpha}\left(e^{\frac{\alpha}{2\kappa}(T-t)} - 1\right),$$

and, using the assumption for υ,

$$\upsilon(t,q) = \frac{\kappa\mu_{\text{ex}}^2}{\alpha^3}\left[\alpha(T-t) + \kappa\left(e^{\frac{\alpha}{\kappa}(T-t)} - 4e^{\frac{\alpha}{2\kappa}(T-t)} + 3\right)\right] + \frac{2\kappa\mu_{\text{ex}}}{\alpha}\left(e^{\frac{\alpha}{2\kappa}(T-t)} - 1\right)q.$$

Remark 1. The special form of the terminal condition for u^{unreg} implies that the optimal strategy of a bank does not depend on its inventory. It follows that the contagion term is independent of the measure flow $m_t(\mathrm{d}q)$, and the forward equation drops from the equation system for the equilibrium. If we consider a slightly more general objective of the form $\max_\nu \mathrm{E}\big(X_T^\nu - \gamma(Q_T^\nu)^2\big)$, the function $\upsilon(t,q)$ becomes quadratic in q and the equilibrium of the MFG is characterized in terms of a forward-backward ODE system, see Cardaliaguet and LeHalle (2018).

4 The case with capital constraints

4.1 The PDE system for an equilibrium

In this section, we derive the coupled PDE system for an equilibrium under regulatory capital constraints.

4.1.1 HJB equation and optimal strategy

With capital constraints, the assumption $u(t,q,x) = x + \upsilon(t,q)$ is inconsistent with the boundary condition for u on $\partial\mathcal{A}$. Moreover, we expect that the optimal trading rate depends on q and x, since banks reduce their position

close to the boundary of $\mathcal{A}$ in order to avoid liquidation. Hence, we need to work with the two-dimensional state price process $\mathbf{X} = (Q, X)$ and with the full HJB equation (3).

To complete the description of the HJB equation in the case with capital constraints, we need to give a precise description of the terminal and boundary conditions that we impose on u. At T, we assume that $u(T, x, q) = x$. Prior to T, we would like to impose the boundary condition $u \equiv 0$ on $\partial\mathcal{A}$. However, this leads to a discontinuity as $t \to T$ as $x = \beta|q| + c > 0$ on $\partial\mathcal{A}$ and hence to problems in the numerics. Hence, we introduce a modified boundary condition as follows: Consider for fixed $0 < \epsilon < T$ a smooth function $k : [0, T] \to \mathbb{R}$ (a regularizer) with the following properties: $k(T) = 1$; $k(t)$ is non-decreasing for all $t \leq T$; $k(t) = 0$ for all $t \leq T - \epsilon$. In the following, we assume that

$$u(t, q, x) = k(t) \cdot (\beta|q| + c), \quad (t, q, x) \in [0, t) \times \partial\mathcal{A}. \tag{14}$$

Condition (14) ensures that $u = 0$ on ∂A for $t < T - \epsilon$ and that at time T, the boundary and terminal conditions are consistent. If a smooth solution u of the HJB equation (3) with the boundary condition (14) exists, the optimal trading rate is by (4) equal to $\nu^*(t, q, x) = \frac{\partial_q u}{2\kappa\partial_x u}(t, x, q)$.

4.1.2 The pre-liquidation distribution

Denote by $\mathbf{X}^{\boldsymbol{\nu}^*}$ the state process given that banks use the strategy $\boldsymbol{\nu}^*$ and that the contagion term $\bar{\mu}_t$ is equal to a known deterministic function $\mu(t)$. Recall the definition of the liquidation time τ (see Section (2.3)) and define for $0 \leq t \leq T$ the *pre-liquidation distribution* $m_t(\mathrm{d}q, \mathrm{d}x)$ of $\mathbf{X}_t^{\boldsymbol{\nu}^*}$ on $\mathcal{A}$ by

$$\langle m_t, f\rangle = \int_{\mathcal{A}} f(q, x) m_t(\mathrm{d}q, \mathrm{d}x) = \mathbb{E}\Big(f\Big(\mathbf{X}_t^{\boldsymbol{\nu}^*}\Big)1_{\{t<\tau\}}\Big),$$

where $f : \mathcal{A} \to \mathbb{R}$ is an arbitrary bounded measurable function. Note that $\langle m_t, 1\rangle = \mathbb{P}(\tau > t)$ gives the proportion of non-liquidated or *active* banks at time t. It follows that for $t > 0$, $\langle m_t, 1\rangle < 1$, that is, m_t is a sub-probability. Denote by $\mathcal{L}_{\mathbf{X}}$ the generator of $\mathbf{X}^{\boldsymbol{\nu}^*}$. For a function f in the domain of $\mathcal{L}_{\mathbf{X}}$ with $f = 0$ on $\partial\mathcal{A}$, the weak form of the forward equation for $m_t(\mathrm{d}q, \mathrm{d}x)$ is

$$\partial_t\langle m_t, f\rangle = \langle m_t, \mathcal{L}_{\mathbf{X}} f\rangle.$$

Integration by parts and the boundary condition $m(t, q, x) \equiv 0$ on $\partial\mathcal{A}$ give the forward equation for the density $m(t, q, x)$ of m_t. It holds that $\partial_t m(t, q, x) = \mathcal{L}_{\mathbf{X}}^* m(t, q, x)$, where $\mathcal{L}_{\mathbf{X}}^*$ is the *adjoint* operator of $\mathcal{L}_{\mathbf{X}}$. More explicitly, one has

$$\partial_t m - \frac{1}{2}\sigma_Q^2\partial_q^2 m - \frac{1}{2}(\sigma_A^2 + \sigma_S^2 q^2)\partial_x^2 m + \partial_q(\nu^* m) + \partial_x\big(\big(q(\mu_{\mathrm{ex}} + \alpha\mu(t)) - \kappa(\nu^*)^2\big)m\big) = 0.$$

The initial condition is $m(0, \cdot) = m_0$ for a given initial density m_0 on $\mathcal{A}$ with $m_0 \equiv 0$ on $\partial\mathcal{A}$.

4.1.3 Contagion term and PDE system

We may now give a formal definition of the contagion term when capital constraints are imposed. Denote—with a slight abuse of notation—the function $(q, x) \mapsto q$ by q. Then

$$\bar{\mu}_t = \partial_t\langle m_t, q\rangle = \partial_t \int_{\mathcal{A}} q \; m_t(\mathrm{d}q, \mathrm{d}x). \tag{15}$$

Note that in (15), we implicitly assume the existence of the derivative $\partial_t\langle m_t, q\rangle$; this property is nontrivial, see Section 4.2.2 for details.

Substituting the relation $\nu^*(t, q, x) = (\partial_q u)/(2\kappa\partial_x u)(t, x, q)$ into the forward equation and using that in equilibrium $\bar{\mu}_t$ and $\mu(t)$ must coincide, we get the following system of coupled PDEs for an equilibrium of the model under capital constraints:

$$
\left.\begin{aligned}
0 &= \partial_t u + q(\mu_{\text{ex}} + \alpha\mu(t))\partial_x u + \frac{1}{2}\sigma_Q^2\partial_q^2 u + \frac{1}{2}(\sigma_A^2 + \sigma_S^2 q^2)\partial_x^2 u + \frac{(\partial_q u)^2}{4\kappa\partial_x u} && \text{(HJB)}\\
0 &= \partial_t m - \frac{1}{2}\sigma_Q^2\partial_q^2 m - \frac{1}{2}(\sigma_A^2 + \sigma_S^2 q^2)\partial_x^2 m + \partial_q\left(\frac{\partial_q u}{2\kappa\partial_x u} m\right)\\
&\quad + \partial_x\left(\left(q(\mu_{\text{ex}} + \alpha\mu(t)) - \frac{(\partial_q u)^2}{4\kappa(\partial_x u)^2}\right)m\right) && \text{(forward)}\\
\mu(t) &= \partial_t \int_{\mathcal{A}} q\ m(t,q,x)\mathrm{d}q\mathrm{d}x && \text{(equilibrium)}\\
u(T,q,x) &= x && \text{(terminal)}\\
m(0,q,x) &= m_0(q,x) && \text{(initial)}\\
u(t,q,x) &= k(t)\cdot(\beta|q| + c) \text{ on } \mathcal{A}^c && \text{(boundary)}\\
m(t,q,x) &= 0 \text{ on } \mathcal{A}^c && \text{(boundary).}
\end{aligned}\right\} \tag{16}
$$

4.2 Discussion of the PDE system

Next we describe qualitative properties of solutions to (16), assuming that a classical solution of the system exists. Moreover, we discuss some of the challenges that arise in the mathematical analysis of the PDE system (16). In this article, we do not provide formal results on existence and uniqueness; in Section 5, we instead use numerical methods to study solutions to the MFG equations (16) from an economic perspective.

4.2.1 Contagion term

We begin with a discussion of the contagion term $\bar{\mu}_t = \partial_t\langle m_t, q\rangle$. Intuitively, there are two sources for contagion: first, the average trading rate of the active banks at t and, second, the amount of assets that are sold in a forced liquidation as banks reach the boundary $\partial\mathcal{A}$. We now give a—somewhat heuristic—mathematical derivation of this decomposition. Suppose that $m(t,q,x)$ is a classical solution of the forward equation that decays exponentially as $|\mathbf{x}| \to \infty$. Denote by $\mathbf{n} = (n_1, n_2)'$ the outer normal to $\partial\mathcal{A}$ and by $\Gamma(\mathrm{d}x, \mathrm{d}q)$ the surface element of $\partial\mathcal{A}$. We have, using first the forward equation for m and second integration by parts and the Gauss–Green theorem (see, for instance, Evans (2010, Appendix C.2)) together with the boundary condition $m \equiv 0$ on $\partial\mathcal{A}$, that

$$
\begin{aligned}
\partial_t\langle m_t, q\rangle &= \int_{\mathcal{A}} q\ \partial_t m(t,q,x)\ \mathrm{d}q\mathrm{d}x = \int_{\mathcal{A}} q\ \mathcal{L}^*_{\mathbf{X}} m(t,q,x)\ \mathrm{d}q\mathrm{d}x\\
&= \int_{\mathcal{A}} m(t,q,x)\mathcal{L}_{\mathbf{X}} q\ \mathrm{d}q\mathrm{d}x + \frac{1}{2}\int_{\partial\mathcal{A}} q\Big(\sigma_Q^2 n_1\partial_Q m + (\sigma_A^2 + q^2\sigma_S^2)n_2\partial_X m\Big)(t,q,x)\ \Gamma(\mathrm{d}q,\mathrm{d}x).
\end{aligned}
$$

Note that in its standard form, the Gauss–Green theorem is valid for compact domains. However, it can be extended to our case using the assumed exponential decay of $m(t,\mathbf{x})$.

Recall that $\mathcal{L}_{\mathbf{X}} q = \nu^*(t,\mathbf{x})$. Hence we get, as $\bar{\mu}_t = \partial_t\langle m_t, q\rangle$,

$$
\bar{\mu}_t = \langle m_t, \nu^*\rangle + \frac{1}{2}\int_{\partial\mathcal{A}} q\Big(\sigma_Q^2 n_1\partial_Q m + (\sigma_A^2 + q^2\sigma_S^2)n_2\partial_X m\Big)(t,q,x)\ \Gamma(\mathrm{d}q,\mathrm{d}x).
$$

The first term is the average trading rate of the active banks, similar to the contagion term in the unregulated case, see (12). The second term gives a mathematical expression for the instantaneous amount of assets that are sold in a forced liquidation. This term is a weighted average of the amount of assets at the liquidation boundary $\partial\mathcal{A}$, with weight function given by

$$
w(t,q,x) = \frac{1}{2}\Big(\sigma_Q^2 n_1\partial_Q m + (\sigma_A^2 + q^2\sigma_S^2)n_2\partial_X m\Big)(t,q,x).
$$

Note that w depends on the generator $\mathcal{L}_{\mathbf{X}}$ only via the diffusion part of $\mathbf{X}$ and not via the drift. Economically, this implies that once a bank is sufficiently close to $\partial\mathcal{A}$, it cannot reduce the probability of liquidation through trading, since the trading rate affects only the drift of the state process. We now provide an interpretation of the form of w. Fix $(\bar{q}, \bar{x}) \in \partial\mathcal{A}$. As shown in Duffie and Lando (2001, Section 2.3), the term

$$\frac{1}{2}(\sigma_A^2 + q^2\sigma_S^2)n_2\ \partial_X m(t, \bar{q}, \bar{x})$$

represents the instantaneous flow through the hyperplane $H = \{(q, \bar{x}) : q \in \mathbb{R}\}$. Multiplication by n_2 selects the component of this flow in the direction of the outward unit normal $\mathbf{n}$ to $\partial\mathcal{A}$ at $(\bar{q}, \bar{x})$, that is, the portion of the flow exiting the domain. An analogous interpretation applies to the term $(1/2)\sigma_Q^2 n_1\ \partial_Q m(t, \bar{q}, \bar{x})$.

4.2.2 Mathematical challenges

Next we discuss mathematical challenges arising in the analysis of the system (16). We begin with the existence of a smooth density of $\mathbf{X}$. If we combine the forward equation for m and the equilibrium condition, we get the following nonlinear and nonlocal differential equation for m:

$$\partial_t m - \frac{1}{2}\sigma_Q^2\partial_q^2 m - \frac{1}{2}(\sigma_A^2 + \sigma_S^2 q^2)\partial_x^2 m + \partial_q\left(\frac{\partial_q u}{2\kappa\partial_x u}m\right) + \partial_x\left(\left(q(\mu_{\text{ex}} + \alpha\partial_t\langle m_t, q\rangle) - \frac{(\partial_q u)^2}{4\kappa(\partial_x u)^2}\right)m\right) = 0.$$

This is the so-called McKean–Vlasov equation for m. The existence of a smooth solution to this equation is not guaranteed. The main problem is the contagion term. If the weight α of the contagion term is relatively large or if many banks are close to the liquidation boundary, the feedback effects due to contagion can lead to a *liquidation cascade*, where a substantial part of the banking system is liquidated simultaneously, so that the mapping $t \mapsto \langle m_t, q\rangle$ has a jump and the contagion term is no longer defined. In the terminology of Nadtochiy and Shkolnikov (2019), this constitutes a *systemic risk event*. In a slightly simpler setting, where X is an uncontrolled one-dimensional process, the existence of solutions to the McKean–Vlasov equation is studied in detail by Delarue et al. (2015) and Hambly et al. (2019). Based on the results obtained in these papers, we conjecture that for α sufficiently large, there will be a systemic risk event, whereas for α sufficiently small, the McKean–Vlasov equation has a smooth solution; this is also in line with the findings from our numerical experiments. Note however, that our setup is more complicated than the models from Delarue et al. (2015) or Hambly et al. (2019) and that the parameters μ_{ex} and κ and the volatility of X and Q play a role as well.

Finally, we comment on the existence of an equilibrium for the MFG, assuming that the McKean–Vlasov equation has a smooth solution. Here, we expect positive results in two cases: a) if the initial distribution m_0 has very little mass close to the liquidation boundary, in other words, if the banking system is well capitalized, the system behaves essentially like the unregulated system for which we have the existence of results; b) if α, κ^{-1}, and T are not too large, we expect existence of a unique solution due to general results on the small-time asymptotics for MFGs. These conjectures are supported by our numerical experiments; a formal analysis is, however, relegated to future research. The work of Burzoni and Campi (2023) might be a good starting point for this.

4.3 Numerical methods for the MFG

In order to solve the coupled PDE system resulting from our MFG numerically, it is necessary to discretize the respective equations. This can be done via finite difference schemes. To solve the resulting discrete system, we use an iterative scheme that consists of Picard iterations. Loosely speaking, one starts with a guess $m^{(0)}$ for the flow of measures, and one computes the associated contagion term $\bar{\mu}^{(0)}$. Then one computes the corresponding solution $u^{(1)}$ and the corresponding strategy $\boldsymbol{\nu}^{(1)}$ of the HJB equation backward in time, using $\bar{\mu}^{(0)}$ as input, and then one determines the dynamics of the corresponding state process $\mathbf{X}^{(1)} = \mathbf{X}^{\boldsymbol{\nu}^{(1)}}$. The measure flow $m^{(1)}$ is then given as the solution of the forward equation for $\mathbf{X}^{(1)}$. From this solution, one computes $\bar{\mu}^{(1)}$, then $u^{(2)}$, and so on, until some convergence criterion is met. Refinements of this approach are discussed in Achdou and Laurière (2020) and in Achdou and Kobeissi (2021).

In Appendix A, we present details of our numerical methodology: we explain how to discretize the system (16) and we give pseudo-code that explains how we implement the Picard iteration. To test our implementation, we compared the theoretical solution for the unregulated case derived in Section 3 to the numerical solution obtained via our implementation of the Picard iteration. The errors obtained were very small; therefore, we feel confident in applying the method to the case with capital constraints as well.

Table 1: Parameter values for the numerical experiments.

Scenario	m_0	α	α_{active}	α_{liq}
1	$\mathcal{N}\left(\begin{pmatrix}5\\60\end{pmatrix}, \begin{pmatrix}0.1 & 0\\0 & 15\end{pmatrix}\right)$	1		
2	$\mathcal{N}\left(\begin{pmatrix}5\\70\end{pmatrix}, \begin{pmatrix}0.1 & 0\\0 & 15\end{pmatrix}\right)$	1		
3	$\mathcal{N}\left(\begin{pmatrix}5\\60\end{pmatrix}, \begin{pmatrix}0.1 & 0\\0 & 15\end{pmatrix}\right)$		1	0.2

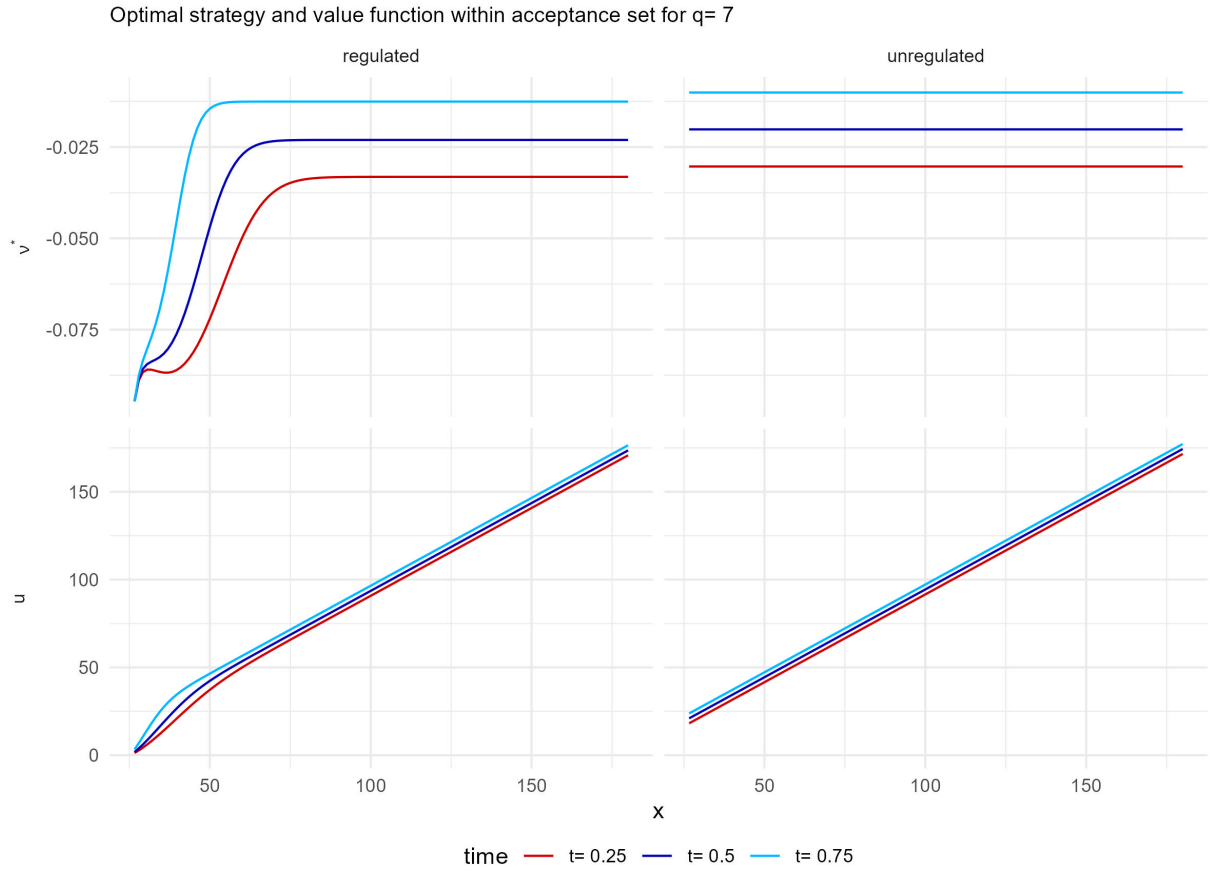

Figure 1: Graph of the optimal strategy (top) and of the value function (bottom) for fixed q and several time points. In the left panels the case with boundary conditions; in the right panels the unregulated case. Parameters are as in Scenario 1 of Table 1. The liquidation boundary for $q = 7$, $c = 5$, and $\beta = 3$ lies at $x = 26$.

5 Numerical experiments for the case with capital constraints

In this section, we report results from numerical experiments. In these experiments, we study how capital constraints affect the trading rate of individual banks and the stability of the banking system. Moreover, we study the effectiveness of two macroprudential risk-management policies, namely (i) increasing the capitalization of the banking system, and (ii) improving the resolution mechanism for banks that violate the capital constraints.

For the numerical solution, we used $N_k = 1000$ time steps, $N_Q = 50$ steps in the q-direction and $N_X = 150$ steps in the x-direction. We fix the parameters $\sigma_Q = 1.4$, $\sigma_S = 2$, $\sigma_A = 0.1$, $\beta = 3$, $c = 5$, $\kappa = 20$, $\mu_{\text{ex}} = -1.6$, and $T = 1$. This parameter setting corresponds to a *recession scenario* where the assets of all banks trend downward ($\mu_{\text{ex}} = -1.6$). Such a scenario is particularly relevant in the context of systemic risk. The remaining parameter values vary across experiments in order to best illustrate certain economic effects and are therefore reported in Table 1.

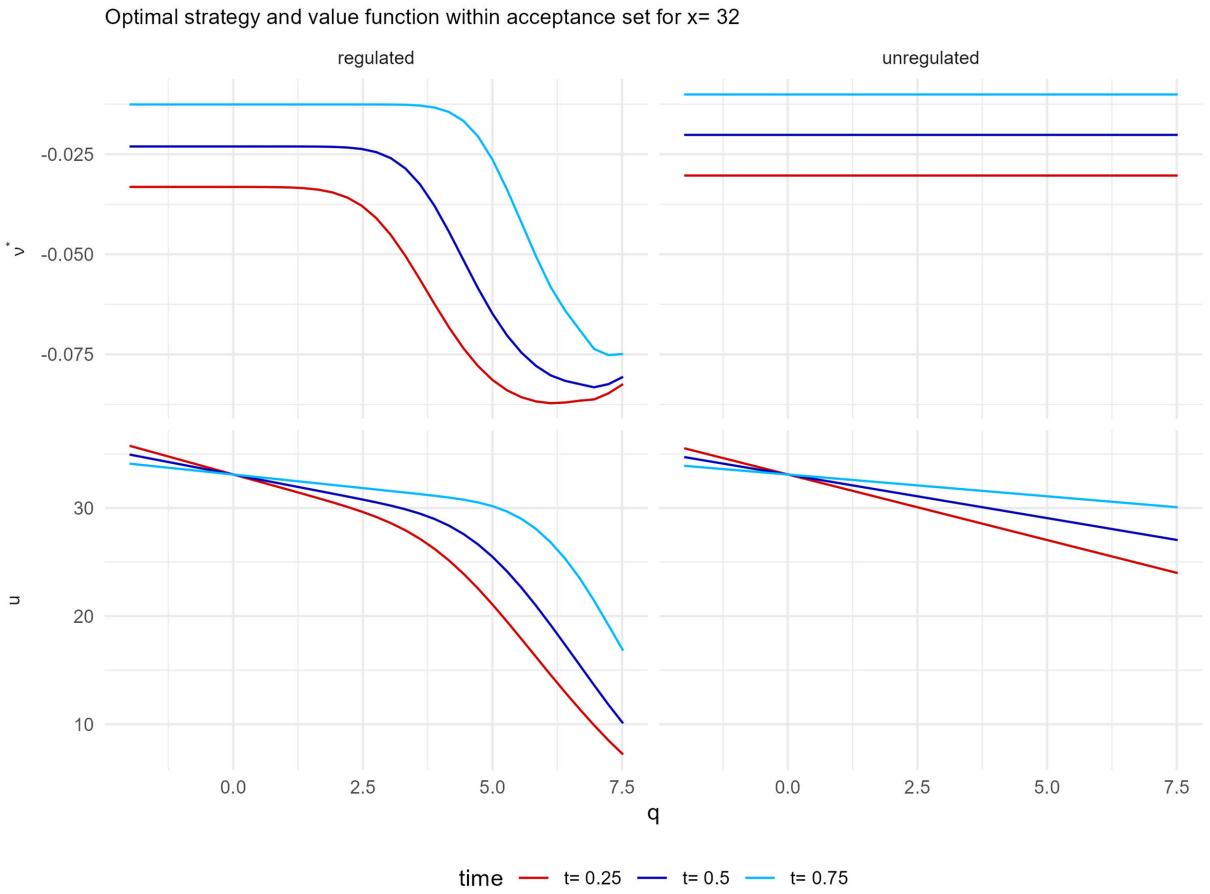

Figure 2: Graph of the optimal strategy (top) and of the value function (bottom) in equilibrium for fixed x and several time points. In the left panels the case with boundary conditions; in the right panels the unregulated case. Parameters are as in Scenario 1 of Table 1.

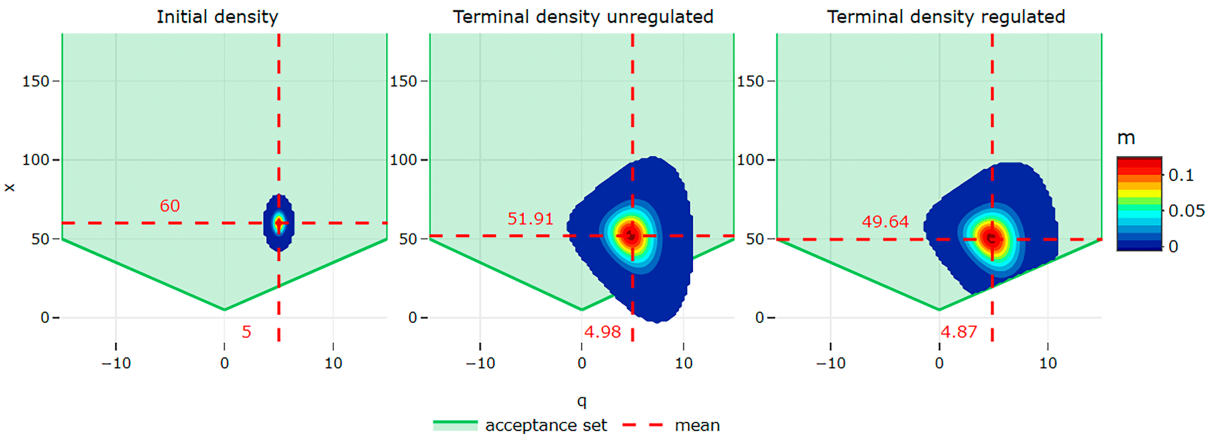

Figure 3: Contour plot of the (sub-)density $m(t, q, x)$ at $t = 0$ and at $t = T$ for the unregulated case (left) and the regulated case (right); acceptance region $\mathcal{A}$ in green, parameters as in Scenario 1 of Table 1.

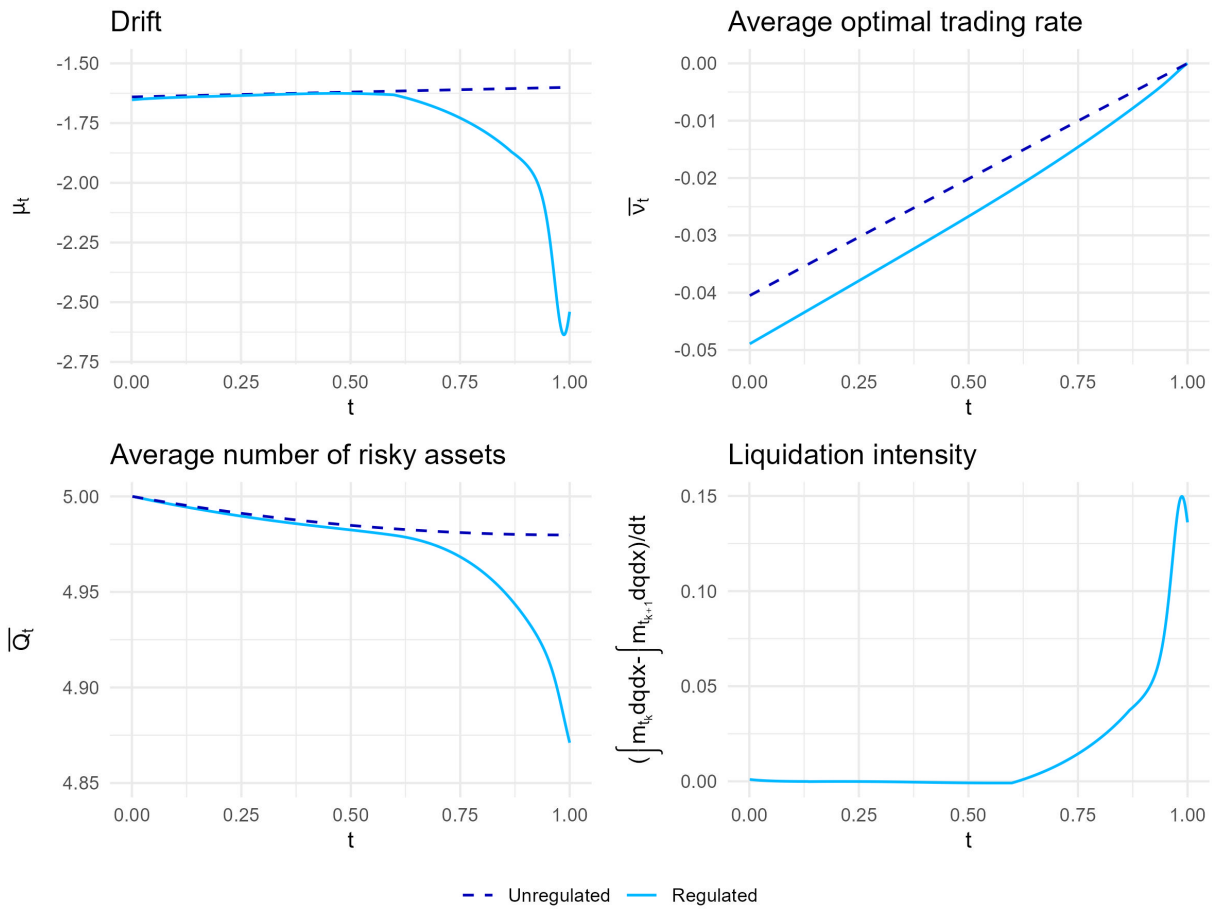

Figure 4: Summary of the banking system. Parameters are as in Scenario 1 of Table 1. Note, in particular, the spike in the liquidation intensity starting at $t = 0.9$.

Remark 2. Our model is highly distorted, so that we have not made an attempt to calibrate parameters to the balance sheet of real banks; instead, we have chosen values with the intention to illustrate the qualitative properties of our model.

5.1 Properties of the optimal trading rate and the value function

In Figure 1, we plot sections of the optimal strategy $\nu^*(t, q, \cdot)$ and of the value function $u(t, q, \cdot)$ for varying x and fixed $q = 7$ for various t. The other parameters are given in the first line of Table 1. Note that $\nu^* < 0$ in the unregulated case, as $\mu_{\text{ex}} < 0$. The left panel corresponds to the case with capital constraints, the right panel gives the solution in the unregulated case. We see that in the presence of capital constraints, for x close to the liquidation boundary, the value function is nonlinear (essentially concave) in x. The optimal trading rate displays an interesting behaviour: for large x, it is constant and slightly lower than the optimal trading rate in the unconstrained case; as x decreases, ν^* decreases substantially because the bank wants to reduce its inventory to avoid liquidation.

In Figure 2, we plot sections of the optimal strategy $\nu^*(t, \cdot, x)$ and of the value function $u(t, \cdot, x)$ for varying q and fixed $x = 32$ for various t. If q is far away from the liquidation boundary, the optimal strategy is constant in the regulated and in the unregulated cases and the value function is linear in both cases. We see that for q close to the liquidation boundary, banks are de-leveraging to avoid liquidation.

5.2 Stability of the banking system

Next we study the impact of capital constraints on the stability of the banking system. The parameters used are given in Scenario 1 of Table 1. In this scenario, at $t = 0$, a large fraction of the banking system is close to the liquidation boundary, due to the low value $\mathrm{E}(X_0) = 60$ for the mean of the initial distribution of banks' equity.

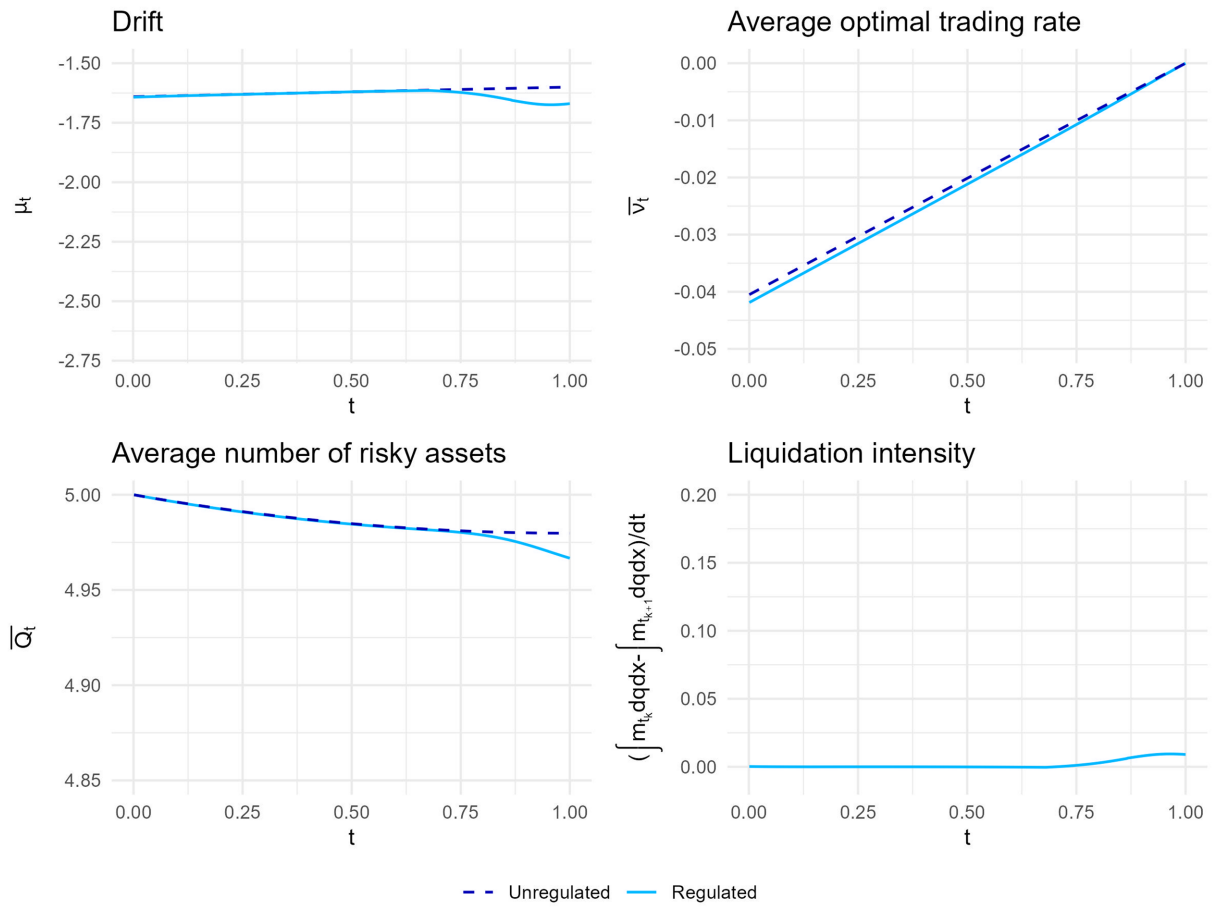

Figure 5: Summary of the banking system with higher initial capital ($\mathbb{E}[X_0] = 70$); other parameters as in Figure 4. Parameters as in Scenario 2 of Table 1.

Figure 3 shows contour plots of the (sub-)density $m(t, q, x)$ at $t = 0$ and $t = T$. Due to the negative drift $\mu_{\text{ex}} = -1.6$, the density curve is transported to the left over time (the average equity value decreases), as we would expect in a recession scenario.

Figure 4 presents a summary of the evolution of the banking system. We observe that there is a strong spike in the liquidation intensity (the change in the proportion of liquidated banks per unit of time) and a strong decrease in $\bar{\mu}_t$ at $t \approx 0.9$, that is, the system is close to a systemic crisis. In fact, if we increase the parameter α, the Picard iterations cease to converge. Further, the plots show that in the regulated case, the risk-bearing capacity of the banking system (the average number of risky assets held by the system) and the mean book value of equity are lower than in the case without capital constraints.

5.3 Macroprudential policy measures

Finally, we analyze the impact of two macroprudential policy measures.

5.3.1 Higher capitalization

It is often argued that a sufficient amount of equity capital in the banking system helps in stabilizing the system, see for instance Admati and Hellwig (2013) or Hanson et al. (2011). We therefore study how a higher level of initial equity relative to the liquidation boundary affects the evolution of the system. In Figure 5, we plot the banking system for the same parameters as in Figure 4 except that we now assume that the mean of the initial equity distribution is $\mathbb{E}(X_0) = 70$ (Scenario 2 of Table 1) and thus substantially higher than in Figure 4. We observe that now the behaviour of the system is very similar to the unregulated case; in particular, the spike in the liquidation intensity starting at $t = 0.9$ has almost disappeared. This clearly supports regulatory efforts to ensure that banking systems are well capitalized.

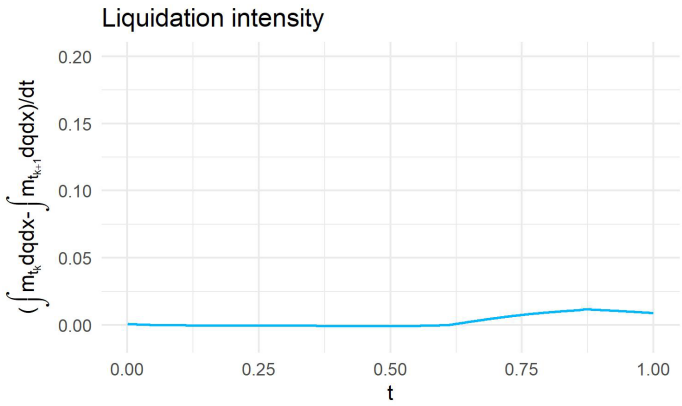

Figure 6: Liquidation intensity with a smaller liquidation impact parameter α_{liq}. Parameters are given in Scenario 3 of Table 1.

5.3.2 Improving the resolution mechanism

The relatively low values for the average trading rate suggest that a systemic risk event is mostly due to the immediate liquidation of banks that breach the capital constraints and less due to the trading behaviour of the active banks. This suggests that financial stability is enhanced if banks violating the capital constraints are resolved in a way that mitigates price-mediated contagion, for instance, by parking the assets of these banks in a special-purpose vehicle that is unwound only gradually over time. A simple way to test this conjecture in our framework is to work with a coefficient α_{active} for the impact of the trading of active banks and with a smaller coefficient α_{liq} for the impact of the liquidation. In Figure 6, we let $\alpha_{\text{active}} = 1$ and $\alpha_{\text{liq}} = 0.2$ (Scenario 3 of Table 1). Figure 6 shows the corresponding liquidation intensity. We see that now the spike in the liquidation intensity disappears. This result supports prudent resolution mechanisms for banks breaching the capital constraints, such as the creation of a special-purpose vehicle where the assets of these banks are parked and sold gradually over time.

Data sharing

No data were analyzed in this article.

Acknowledgements

We would like to thank Yves Achdou for his helpful comments regarding the numerical solution of our PDE system. Open Access funding provided by Wirtschaftsuniversitat Wien/KEMÖ.

ORCID

Rüdiger Frey: https://orcid.org/0000-0002-8402-4653
Theresa Traxler: https://orcid.org/0009-0005-9652-5147

A Details on the numerical implementation

A1 Overview and notation

Our goal is to numerically solve the coupled PDE system (16) by first discretizing it and then using Picard iterations, where the value function and density describing the system are updated until convergence. The main challenges in solving the system numerically are (i) the coupling between the HJB and the forward equation, (ii) the fact that the HJB equation goes backward in time while the PDE describing the evolution of the density goes forward in time, (iii) the natural requirement for the density to be nonnegative and mass-preserving, and (iv) the nonlinearity of our system with respect to various partial derivatives. One common approach from the literature to overcome the first three challenges is to use a special finite-difference scheme consisting of a combination of right- and left-sided differences combined with Picard iterations until convergence of the

system. We briefly describe how we tackle the last challenge mentioned, which arises from the structure of our PDE system. For completeness, let us start by introducing some standard notation needed for the discretization of the system.

For positive integers N_T, N_Q, and N_X, we define the time step size as

$$\Delta t = \frac{T}{N_T},$$

and the step size related to the state variables Q and X as

$$\Delta q = \frac{Q_{\max} - Q_{\min}}{N_Q},$$

and

$$\Delta x = \frac{X_{\max} - X_{\min}}{N_X},$$

respectively. The set of discrete time steps on our grid is then $\mathfrak{T} = \{t_k = k\Delta t, k = 0, \dots, N_T\}$ and the grid corresponding to the state variable is $\mathfrak{H} = \{h_{ij} = (q_i, x_j) = (Q_{\min} + i\Delta q, X_{\min} + j\Delta x), i = 0, \dots, N_Q, j = 0, \dots, N_X\}$. We aim to approximate $u(t_k, h_{i,j})$ and $m(t_k, h_{i,j})$ by $u^k_{i,j}$ and $m^k_{i,j}$, respectively, through solving the discrete approximations of the coupled PDE system. We define the following finite-difference operators for some function $y : \mathfrak{T} \times \mathfrak{H} \to \mathbb{R}$:

$$D_t y^k_{i,j} = \frac{y^{k+1}_{i,j} - y^k_{i,j}}{\Delta t}, \qquad \text{[Discrete time derivative]}$$

$$D_q y^k_{i,j} = \frac{y^k_{i+1,j} - y^k_{i-1,j}}{2\Delta q}, \qquad \text{[Central difference operator in } q\text{]}$$

$$D^R_q y^k_{i,j} = \frac{y^k_{i+1,j} - y^k_{i,j}}{\Delta q}, \qquad \text{[Right difference operator in } q\text{]}$$

$$D^L_q y^k_{i,j} = \frac{y^k_{i,j} - y^k_{i-1,j}}{\Delta q}, \qquad \text{[Left difference operator in } q\text{]}$$

$$D_x y^k_{i,j} = \frac{y^k_{i,j+1} - y^k_{i,j-1}}{2\Delta x}, \qquad \text{[Central difference operator in } x\text{]}$$

$$\Delta_q y^k_i = -\frac{1}{\Delta q^2}\left(2y^k_{i,j} - y^k_{i+1,j} - y^k_{i-1,j}\right), \qquad \text{[Central second order difference in } q\text{]}$$

$$\Delta_x y^k_{i,j} = -\frac{1}{\Delta x^2}\left(2y^k_{i,j} - y^k_{i,j+1} - y^k_{i,j-1}\right), \qquad \text{[Central second order difference in } x\text{]}$$

$$\Delta_{qx} y^k_{i,j} = \frac{D_q y^k_{i,j+1} - D_q y^k_{i,j-1}}{2\Delta x} = \frac{y^k_{i+1,j+1} - y^k_{i-1,j+1} - y^k_{i+1,j-1} + y^k_{i-1,j-1}}{\Delta q \Delta x}. \qquad \text{[Mixed second order difference]}$$

By definition of these operators, at boundary nodes, the grid needs to be extended by one layer. We extend both the value function and the density linearly, that is, by assuming $u(q + \Delta q, x) = u(q, x) + (u(q, x) - u(q - \Delta q, x))$, $u(q, x + \Delta x) = u(q, x) + (u(q, x) - u(q, x - \Delta x))$, and assuming about m similarly. Before discretizing our equation system, we also need to rewrite some terms. Note that

$$\partial_q\left(\frac{\partial_q u}{2\kappa\partial_x u}m\right) = \partial_q\left(\frac{\partial_q u}{2\kappa\partial_x u}\right)m + \frac{\partial_q u}{2\kappa\partial_x u}\partial_q m = \frac{1}{2\kappa}\frac{\partial_q^2 u\partial_x u - \partial_q u\partial_q\partial_x u}{(\partial_x u)^2}m + \frac{\partial_q u}{2\kappa\partial_x u}\partial_q m$$

and

$$\partial_x\left(\left(q(\mu_{\text{ex}}+\alpha\mu)-\frac{(\partial_q u)^2}{4\kappa(\partial_x u)^2}\right)m\right)=q(\mu_{\text{ex}}+\alpha\mu)\partial_x m-\partial_x\left(\frac{(\partial_q u)^2}{4\kappa(\partial_x u)^2}\right)m-\frac{(\partial_q u)^2}{4\kappa(\partial_x u)^2}\partial_x m$$

$$=q(\mu_{\text{ex}}+\alpha\mu)\partial_x m-\frac{1}{4\kappa}\frac{\partial_x(\partial_q u)^2\cdot(\partial_x u)^2-(\partial_q u)^2\cdot\partial_x(\partial_x u)^2}{(\partial_x u)^4}m-\frac{(\partial_q u)^2}{4\kappa(\partial_x u)^2}\partial_x m$$

$$=q(\mu_{\text{ex}}+\alpha\mu)\partial_x m-\frac{1}{4\kappa}\frac{2\partial_q u\partial_x\partial_q u\cdot(\partial_x u)^2-(\partial_q u)^2\cdot 2\partial_x u\partial_x^2 u}{(\partial_x u)^4}m-\frac{(\partial_q u)^2}{4\kappa(\partial_x u)^2}\partial_x m.$$

A2 Discretization

In what follows, with regards to the discretization of the system, we follow the idea proposed by Achdou and Laurière (2020), who use a mix of right- and left-sided difference operators for the discretization in order to be able to overcome the challenges (i)–(iii). A numerical Hamiltonian is used that is non-increasing in the right-sided differences and non-decreasing in the left-sided differences of the state variable.

However, we need to modify this idea due to the complexity of our model. In our PDE system, there are terms whose monotonicity with respect to derivatives in different dimensions is not clear, as they depend on derivatives with respect to both q and x. We therefore use central difference operators in x, but distinguish between left- and right-sided difference operators in the dimension of q in order to overcome challenge (iv). Thereby, we can achieve better stability of our algorithm. Specifically, we choose the numerical Hamiltonian such that it is non-increasing in the right-sided difference D_q^R and non-decreasing in the left-sided difference D_q^L.

We discretize the term

$$\frac{(\partial_q u)^2}{4\kappa\partial_x u}$$

in the HJB as

$$\max\left\{\frac{\left[\left(D_q^R u_{i,j}^k\right)^-\right]^2}{4\kappa D_x u_{i,j}^k},\frac{\left[\left(D_q^L u_{i,j}^k\right)^+\right]^2}{4\kappa D_x u_{i,j}^k}\right\}.$$

For the forward equation, we discretize the term

$$\partial_q\left(\frac{\partial_q u}{2\kappa\partial_x u}m\right)=\frac{1}{2\kappa}\frac{\partial_q^2 u\partial_x u-\partial_q u\partial_q\partial_x u}{(\partial_x u)^2}m+\frac{\partial_q u}{2\kappa\partial_x u}\partial_q m$$

as

$$\frac{1}{2\kappa}\frac{\Delta_q u_{i,j}^k D_x u_{i,j}^k-\left\{\max\left[\left(D_q^R u_{i,j}^k\right)^+\left(\Delta_{qx}u_{i,j}^k\right)^+,\left(D_q^L u_{i,j}^k\right)^-\left(\Delta_{qx}u_{i,j}^k\right)^-\right]+\min\left[\left(D_q^R\,u_{i,j}^k\right)^-\left(\Delta_{qx}u_{i,j}^k\right)^+,\left(D_q^L u_{i,j}^k\right)^+\left(\Delta_{qx}u_{i,j}^k\right)^-\right]\right\}}{\left(D_x u_{i,j}^k\right)^2}m_{i,j}^k$$

$$+\frac{1}{2\kappa D_x u_{i,j}^k}\Big[\max\left\{(D_q^L\,u_{i,j}^k)^+(D_q^L m_{i,j}^k)^+,(D_q^R u_{i,j}^k)^-(D_q^R m_{i,j}^k)^-\right\}+\min\left\{(D_q^R\,u_{i,j}^k)^+(D_q^L m_{i,j}^k)^-,(D_q^L u_{i,j}^k)^-(D_q^R m_{i,j}^k)^+\right\}\Big],$$

and the term

$$\partial_x\left(\left(q(\mu_{\text{ex}}+\alpha\mu)-\frac{(\partial_q u)^2}{4\kappa(\partial_x u)^2}\right)m\right)$$

$$=q(\mu_{\text{ex}}+\alpha\mu)\partial_x m-\frac{1}{4\kappa}\frac{2\partial_q u\partial_x\partial_q u\cdot(\partial_x u)^2-(\partial_q u)^2\cdot 2\partial_x u\partial_x^2 u}{(\partial_x u)^4}m-\frac{(\partial_q u)^2}{4\kappa(\partial_x u)^2}\partial_x m,$$

as

$$
\begin{aligned}
&q(\mu_{ex}+\alpha\mu^k+\delta)D_x m^k_{i,j}\\
&\quad -\frac{1}{4\kappa}\frac{\begin{array}{c}2\left(D_x u^k_{i,j}\right)^2\Big\{\max\left[\left(D^L_q\, u^k_{i,j}\right)^+\left(\Delta_{qx}u^k_{i,j}\right)^+,\left(D^R_q u^k_{i,j}\right)^-\left(\Delta_{qx}u^k_{i,j}\right)^-\right]\\ +\min\left[\left(D^L_q\, u^k_{i,j}\right)^-\left(\Delta_{qx}u^k_{i,j}\right)^+,\left(D^R_q u^k_{i,j}\right)^+\left(\Delta_{qx}u^k_{i,j}\right)^-\right]\Big\}\end{array}}{(D_x u^k_{i,j})^4}m^k_{i,j}\\
&\quad +\frac{1}{4\kappa}\frac{\max\left\{\left[\left(D^R_q\, u^k_{i,j}\right)^-\right]^2,\left[\left(D^L_q u^k_{i,j}\right)^+\right]^2\right\}\cdot 2D_x u^k_{i,j}\Delta_x u^k_{i,j}}{(D_x u^k_{i,j})^4}m^k_{i,j}-\max\left\{\frac{\left[\left(D^L_q u^k_{i,j}\right)^-\right]^2}{4\kappa\left(D_x u^k_{i,j}\right)^2},\frac{\left[\left(D^R_q u^k_{i,j}\right)^+\right]^2}{4\kappa\left(D_x u^k_{i,j}\right)^2}\right\}D_x m^k_{i,j}.
\end{aligned}
$$

To shorten the notation, we define

$$
\begin{aligned}
&F_{ij}(u^k,m^k):=\frac{1}{2\kappa}\Bigg(\frac{\Delta_q u^k_{i,j}D_x u^k_{i,j}}{\left(D_x u^k_{i,j}\right)^2}\\
&-\frac{\max\left[\left(D^R_q u^k_{i,j}\right)^+\left(\Delta_{qx}u^k_{i,j}\right)^+,\left(D^L_q u^k_{i,j}\right)^-\left(\Delta_{qx}u^k_{i,j}\right)^-\right]+\min\left[\left(D^R_q\, u^k_{i,j}\right)^-\left(\Delta_{qx}u^k_{i,j}\right)^+,\left(D^L_q u^k_{i,j}\right)^+\left(\Delta_{qx}u^k_{i,j}\right)^-\right]}{(D_x u^k_{i,j})^2}\Bigg)m^k_{i,j}\\
&+\frac{1}{2\kappa D_x u^k_{i,j}}\Big[\max\left\{(D^L_q\, u^k_{i,j})^+(D^L_q m^k_{i,j})^+,(D^R_q u^k_{i,j})^-(D^R_q m^k_{i,j})^-\right\}\\
&+\min\left\{(D^R_q\, u^k_{i,j})^+(D^L_q m^k_{i,j})^-,(D^L_q u^k_{i,j})^-(D^R_q m^k_{i,j})^+\right\}\Big]+q(\mu_{ex}+\alpha\mu^k+\delta)D_x m^k_{i,j}\\
&\quad -\frac{\begin{array}{c}2\left(D_x u^k_{i,j}\right)^2\cdot\Big\{\max\left[\left(D^L_q\, u^k_{i,j}\right)^+\left(\Delta_{qx}u^k_{i,j}\right)^+,\left(D^R_q u^k_{i,j}\right)^-\left(\Delta_{qx}u^k_{i,j}\right)^-\right]\\ +\min\left[\left(D^L_q\, u^k_{i,j}\right)^-\left(\Delta_{qx}u^k_{i,j}\right)^+,\left(D^R_q u^k_{i,j}\right)^+\left(\Delta_{qx}u^k_{i,j}\right)^-\right]\Big\}\end{array}}{4\kappa(D_x u^k_{i,j})^4}m^k_{i,j}\\
&+\frac{\max\left\{\left[\left(D^R_q\, u^k_{i,j}\right)^-\right]^2,\left[\left(D^L_q u^k_{i,j}\right)^+\right]^2\right\}\cdot 2D_x u^k_{i,j}\Delta_x u^k_{i,j}}{4\kappa(D_x u^k_{i,j})^4}m^k_{i,j}-\max\left\{\frac{\left[\left(D^L_q u^k_{i,j}\right)^-\right]^2}{4\kappa\left(D_x u^k_{i,j}\right)^2},\frac{\left[\left(D^R_q u^k_{i,j}\right)^+\right]^2}{4\kappa\left(D_x u^k_{i,j}\right)^2}\right\}D_x m^k_{i,j},
\end{aligned}
$$

which leads to the following discretized PDE system.

$$
\begin{cases}
D_t u^k_{i,j}+q_i(\mu_{\text{ex}}+\alpha\mu^k)D_x u^k_{i,j}+\frac{1}{2}\sigma_Q^2\Delta_q u^k_{i,j}+\frac{1}{2}(\sigma_A^2+\sigma_S^2 q_i^2)\Delta_x u^k_{i,j}\\
\quad+\max\left\{\frac{\left[\left(D^R_q u^k_{i,j}\right)^-\right]^2}{4\kappa D_x u^k_{i,j}},\frac{\left[\left(D^L_q u^k_{i,j}\right)^+\right]^2}{4\kappa D_x u^k_{i,j}}\right\}=0,\\
D_t m^k_{i,j}-\frac{1}{2}\sigma_Q^2\Delta_q m^k_{i,j}-\frac{1}{2}(\sigma_A^2+\sigma_S^2 q^2)\Delta_x m^k_{i,j}+F_{i,j}(u^k,m^k)=0\\
\mu^k=D_t\left(\sum_i\sum_j q_i m^k_{i,j}\Delta x\Delta q\right),\\
u(T,q_i,x_j)=x_j-\gamma q_i^2,\\
m(0,q_i,x_j)=m_0(x_i,q_j),\\
u(t_k,q_i,x_j)\equiv k(t_k)\cdot(\beta q_i+c)\text{ on }\mathcal{A}^c,\\
m(t_k,q_i,x_j)\equiv 0\text{ on }\mathcal{A}^c.
\end{cases}
$$

A3 Picard iteration

The discretized PDE system can now be used to update initial guesses of the value function u (backward in time) and the density m (forward in time) iteratively, until a convergence criterion is met.

We implement these Picard iterations in R. The following pseudo code shows the structure of the algorithm.

Iterative Solvers	
function `iterate`$_{\mathtt{u}}$`(u,m)`	iteration of u
for $k = N_T - 1, \dots, 1$	backward iteration
$l = 0$	
$u^0 = u$	
$\mu^k = D_t\left(\sum_i \sum_j q_i m_{i,j}^k \Delta x \Delta q\right)$	drift
while error > tolerance	
$l = l + 1$	iteration step
$u_{ij}^{k,l} = u_{ij}^{k+1,l} + \Delta t \cdot \Bigg[q_i(\mu_{\text{ex}} + \alpha\mu^k) D_x u_{i,j}^{k,l} + \frac{1}{2}\sigma_Q^2 \Delta_q u_{i,j}^{k,l}$	updated value function
$+ \frac{1}{2}(\sigma_A^2 + \sigma_S^2 q_i^2)\Delta_x u_{i,j}^{k,l} + \max\left\{ \frac{\left[\left(D_q^R u_{i,j}^{k,l}\right)^-\right]^2}{4\kappa D_x u_{i,j}^{k,l}}, \frac{\left[\left(D_q^L u_{i,j}^{k,l}\right)^+\right]^2}{4\kappa D_x u_{i,j}^{k,l}} \right\} \Bigg]$	
if regulated = TRUE $\quad u_{ij}^{k,l}[\mathcal{A}^c] = k(t_k) \cdot (\beta q_i + c)$	boundary condition
error = mean(abs($u_{ij}^{k,l} - u_{ij}^{k,l-1}$))	error between guesses
return u	
function `iterate`$_{\mathtt{m}}$`(u,m)`	iteration of m
for $k = 1, \dots, N_T - 1$	forward iteration
$p = 0$	
$m^0 = m$	
while error > tolerance	
$\mu^{k,p} = D_t\left(\sum_i \sum_j q_i m_{i,j}^{k,p} \Delta x \Delta q\right)$	drift
$p = p + 1$	iteration step
$m_{ij}^{k+1,p} = m_{ij}^{k,p} - \Delta t\left[-\frac{1}{2}\sigma_Q^2 \Delta_q m_{i,j}^{k,p} - \frac{1}{2}(\sigma_A^2 + \sigma_S^2 q^2)\Delta_x m_{i,j}^{k,p} + F_{ij}(u^{k,p}, m^{k,p})\right]$	updated density
if regulated = TRUE $m_{ij}^{k+1,p}[\mathcal{A}^c] = 0$	boundary condition
error = mean(abs($m_{ij}^{k+1,p} - m_{ij}^{k+1,p-1}$))	error between guesses
return m	

Picard Iteration	
$u = u_T, m = m_0$	initialization
$n = 0$	iteration step
while error > tolerance	iteration on whole grid
$n = n + 1$	iteration step
$u =$ `iterate`$_{\mathtt{u}}$`(u,m)`	iteration of u
$m =$ `iterate`$_{\mathtt{m}}$`(u,m)`	iteration of m
error = $\left[\text{mean}(\text{abs}(u_{ij}^{k,n} - u_{ij}^{k,n-1})) + \text{mean}(\text{abs}(m_{ij}^{k,n} - m_{ij}^{k,n-1}))\right]/2$	error between guesses

References

Achdou, Y. and Kobeissi, Z. (2021). Mean field games of controls: Finite difference approximations. *Mathematics in Engineering*, 3(3):1–35. doi: 10.3934/mine.2021024.

Achdou, Y. and Laurière, M. (2020). Mean field games and applications: Numerical aspects. arXiv preprint arXiv:2003.04444.

Admati, A. and Hellwig, M. (2013). *The Bankers' New Clothes: What's Wrong with Banking and What to Do About It*, Princeton University Press, Princeton, NJ.

Banerjee, T. and Feinstein, Z. (2021). Price mediated contagion through capital ratio requirements with VWAP liquidation prices. *European Journal of Operational Research*, 295(3):1147–1160. doi: 10.1016/j.ejor.2021.03.053.

Basel Committee on Banking Supervision (2014). *Basel III Leverage Ratio Framework and Disclosure Requirements*, Bank of International Settlements, Basel, Switzerland. https://www.bis.org/publ/bcbs270.htm.

Bayraktar, E., Guo, G., Tang, W., and Zhang, Y. P. (2023). Systemic robustness: A mean-field particle system approach. arXiv preprint arXiv:2212.08518.

Braouezec, Y. and Wagalath, L. (2018). Risk-based capital requirements and optimal liquidation in a stress scenario. *Review of Finance*, 22(2):747–782. doi: 10.1093/rof/rfw067.

Braouezec, Y. and Wagalath, L. (2019). Strategic fire-sales and price-mediated contagion in the banking system. *European Journal of Operational Research*, 274(3):1180–1197. doi: 10.1016/j.ejor.2018.11.012.

Burzoni, M. and Campi, L. (2023). Mean field games with absorption and common noise with a model of bank run. *Stochastic Processes and Their Applications*, 164:206–241. doi: 10.1016/j.spa.2023.07.007.

Campi, L. and Fischer, M. (2018). N-player games and mean field games with absorption. *The Annals of Applied Probability*, 28(4):2188–2242. doi: 10.1214/17-AAP1354.

Cardaliaguet, P. and LeHalle, C. A. (2018). Mean field game of controls and an application to trade crowding. *Mathematics and Financial Economics*, 12:335–363.

Cardaliaguet, P. and Porretta, A. (Eds.), (2019). *Mean Field Games*, Lecture Notes in Mathematics, Vol. 2281, Springer Nature, Cham, Switzerland.

Carmona, R. and Delarue, F. (2018). *Probabilistic Theory of Mean Field Games With Applications I-II*, Springer International Publishing, Cham, Switzerland.

Carmona, R., Fouque, J.-P., and Sun, L.-H. (2015). Mean-field games and systemic risk. *Communications in Mathematical Sciences*, 13(4):911–933. doi: 10.4310/CMS.2015.v13.n4.a4.

Cartea, Á., Jaimungal, S., and Penalva, J. (2015). *Algorithmic and High-Frequency Trading*, Cambridge University Press, Cambridge, United Kingdom.

Casgrain, P. and Jaimungal, S. (2020). Mean-field games with differing beliefs for algorithmic trading. *Mathematical Finance*, 30(3):995–1034. doi: 10.1111/mafi.12237.

Cont, R. and Schaanning, E. (2019). Monitoring indirect contagion. *Journal of Banking and Finance*, 104:85–102. doi: 10.1016/j.jbankfin.2019.04.007.

Cont, R. and Wagalath, L. (2016). Fire sales forensics: Measuring endogenous risk. *Mathematical Finance*, 26(4):835–866. doi: 10.1111/mafi.12071.

Cuchiero, C., Reisinger, C., and Rigger, S. (2024). Optimal bailout strategies resulting from the drift controlled supercooled Stefan problem. *Annals of Operations Research*, 336(1):1315–1349. doi: 10.1007/s10479-023-05293-7.

Cuchiero, C., Rigger, S., and Svaluto-Ferro, S. (2023). Propagation of minimality in the supercooled Stefan problem. *The Annals of Applied Probability*, 33(2):1588–1618. doi: 10.1214/22-AAP1850.

Daníelsson, J., Embrechts, P., Goodhart, C., Keating, C., Muennich, F., and Renault, O. (2001). *An Academic Response to Basel II. Special Paper No. 130*, Financial Markets Group, London School of Economics, London, United Kingdom.

Delarue, F., Inglis, J., Rubenthaler, S., and Tanré, E. (2015). Global solvability of a networked integrate-and-fire model of McKean-Vlasov type. *The Annals of Applied Probability*, 25(4):2096–2133. doi: 10.1214/14-AAP1044.

Duffie, D. and Lando, D. (2001). Term structure of credit risk with incomplete accounting observations. *Econometrica*, 69:633–664.

Eisenberg, L. and Noe, T. H. (2001). Systemic risk in financial systems. *Management Science*, 47(2):236–249.

Elsinger, H., Lehar, A., and Summer, M. (2006). Risk assessment for banking systems. *Management Science*, 52:1301–1314.

Evans, L. C. (2010). *Partial Differential Equations, 19 of Graduate Studies in Mathematics*, 2nd ed., American Mathematical Society, Providence, RI.

Feinstein, Z. (2020). Capital regulation under price impacts and dynamic financial contagion. *European Journal of Operational Research*, 281(2):449–463. doi: 10.1016/j.ejor.2019.08.044.

Frey, R. and Hledik, J. (2018). Diversification and systemic risk: a financial network perspective. *Risks*, 6(2):54.

Glasserman, P. and Young, H. P. (2016). Contagion in financial networks. *Journal of Economic Literature*, 54(3):779–831. doi: 10.1257/jel.20151228.

Hambly, B. and Jettkant, P. (2023). Control of McKean–Vlasov SDEs with contagion through killing at a state-dependent intensity. arXiv preprint arXiv:2310.15854

Hambly, B., Ledger, S., and Søjmark, A. (2019). A McKean–Vlasov equation with positive feedback and blow-ups. *The Annals of Applied Probability*, 29(4):2338–2373.

Hambly, B. and Søjmark, A. (2019). An SPDE model for systemic risk with endogenous contagion. *Finance and Stochastics*, 23:535–594. doi: 10.1007/s00780-019-00396-1.

Hanson, S., Kashyap, A., and Stein, J. (2011). A macroprudential approach to financial regulation. *Journal of Economic Perspectives*, 25(1):3–28.

Lasry, J.-M. and Lions, P.-L. (2006a). Jeux à champ moyen. II - Horizon fini et contrôle optimal. *Comptes Rendus Mathematique*, 343:679–684. doi: 10.1016/j.crma.2006.09.018.

Lasry, J.-M. and Lions, P.-L. (2006b). Théorie des jeux/Économie mathématique. *Comptes Rendus Mathematique*, 343(9):619–625. doi: 10.1016/j.crma.2006.09.019.

Ledger, S. and Søjmark, A. (2020). Uniqueness for contagious McKean–Vlasov systems in the weak feedback regime. *Bulletin of the London Mathematical Society*, 52(3):448–463. doi: 10.1112/blms.12337.

McNeil, A. J., Frey, R., and Embrechts, P. (2015). *Quantitative Risk Management: Concepts, Techniques and Tools*, 2nd ed., Princeton University Press, Princeton.

Nadtochiy, S. and Shkolnikov, M. (2019). Particle systems with singular interaction through hitting times: Application in systemic risk modeling. *The Annals of Applied Probability*, 29:89–129.

Pham, H. (2009). *Continuous-Time Stochastic Control and Optimization with Financial Applications. No. 61 in Stochastic Modelling and Applied Probability*, Springer, Berlin.

Rogers, L. and Veraart, L. (2013). Failure and rescue in an interbank network. *Management Science*, 59:882–898.

Received 22 April 2025 — Accepted 29 November 2025